Article **Journal Civil Engineering**
June 2021, Vol.5 No.13 31-44

Stress concentration in a plate with two centered holes subjected to axial loading

Concentración de esfuerzos en una placa con dos barrenos centrados sometida a carga axial

ORTEGA, Francisco†, PALACIOS, Francisco, GARCIA, Diego and GARCIA, José

Instituto Tecnológico Superior de Irapuato. Irapuato Silao Highway km 12.5 CP 36821 Irapuato, Gto., Mexico.

ID 1st Author: *Francisco, Ortega*

ID 1st Co-author: *Francisco, Palacios*

ID 2nd Co-author: *Diego, Garcia*

ID 3rd Co-author: *José. Garcia*

DOI: 10.35429/JCE.2021.13.5.31.44 Received 25 January, 2021; Accepted 30 June, 2021

Abstract

In the present work the stress concentration in a flat plate subjected to axial load is analyzed. To carry out this analysis, the stress concentration factor is determined with the help of the Ansys software, which uses the finite element theory to carry out its analyses. A total of 125 simulations are performed, obtaining the maximum stresses that support the piece, which are used to determine the stress concentration factor. Stress concentration factors are plotted as a function of S/D (hole center distance/hole diameter) for W/D (part thickness/hole diameter) ratios of 1.2, 1.5, 2, 2.5, 3. The graphed results are regressed using the method of least squares to obtain equations that can be used to predict the stress concentration factor of this type of mechanical parts. The equations obtained are sets of linear, exponential, and polynomial equations with correlation coefficient values that vary from 0.8835 to 0.9997.

Concentration, Efforts, Factor

Resumen

En el presente trabajo se analiza la concentración de tensiones en una placa plana sometida a una carga axial. Para realizar este análisis se determina el factor de concentración de tensiones con la ayuda del software Ansys, que utiliza la teoría de elementos finitos para realizar sus análisis. Se realizan un total de 125 simulaciones, obteniendo las tensiones máximas que soporta la pieza, que se utilizan para determinar el factor de concentración de tensiones. Los factores de concentración de tensiones se grafican en función de S/D (distancia entre centros de agujeros/diámetro de agujeros) para relaciones W/D (espesor de la pieza/diámetro de agujeros) de 1.2, 1.5, 2, 2.5, 3. Los resultados graficados se regresan utilizando el método de los mínimos cuadrados para obtener ecuaciones que puedan ser utilizadas para predecir el factor de concentración de tensiones de este tipo de piezas mecánicas. Las ecuaciones obtenidas son conjuntos de ecuaciones lineales, exponenciales y polinómicas con valores de coeficientes de correlación que varían entre 0,8835 y 0,9997.

Concentración, Esfuerzos, Factor

Citation: ORTEGA, Francisco, PALACIOS, Francisco, GARCIA, Diego and GARCIA, José. Stress concentration in a plate with two centered holes subjected to axial loading. Journal Civil Engineering. 2021. 5-13:31-44.

† Researcher contributing as first author.

Nomenclature

The nomenclature used during the development of this work is shown below.

TO	Cross-sectional area of the plate
B.	Deformation matrix
D	Hole diameter
F	Force applied to part
H1.2	Quadrature Weight Coefficients gaussian
J	Jack o biano
Kand	stiffness matrix
Kyou	Fact stress concentration tower
L	Plate length
N	Matrix of form functions
Ni…p	Fan form of node i, j, k, l, *m, n, o, p* belonging to the square element
Rtwo	Correlation coefficient
s	Separation between the centers of the drill holes
W	Plate width
x	Element global coordinate
Y	Element global coordinate
η	Local coordinate of the element
ξ	Local coordinate of the element
σmax	Maximum effort
σtheoreti	Theoretical effort

Introduction

The stress concentration is one of the main problems that designers must worry about when designing any type of machinery or equipment, because stress concentrations can cause the different mechanical parts to fracture and the machine or equipment to lose its operating conditions. For this reason, designers should try to eliminate stress concentrators in mechanical parts as much as possible.

Special attention must be paid to analyze the stress concentrators in the best possible way so that the designs that are made work properly and are as reliable as possible.

Many researchers have studied different types of stress concentrators and the effect they have on different materials. Zheng & Niemi (1997) investigates the relationship between stress and local strain, as well as the nominal stress proposed by Moski and Glinka.

The authors comment that said stress is good for low stress amplitudes, however both the Neuber rule and the Moski and Glinka methods do not produce good results for large stress amplitudes. For their part, Roldan & Bastidas (2002) present a study which analyzes the stress concentration on a flat plate of constant thickness subjected to stress at its ends, making a comparison of the results obtained through the theory of elasticity, experimentally and by the finite element method.

Maíz, Rossi, Laura & Bambill (2004) comment that the normal stresses increase in absolute value with the size of the hole for all orthotropic materials. For their part, Bambill, Susca, Laura & Maíz (2005) mention that the stresses generated in the environment of a circular hole of an orthotropic plate when it is subjected to hydrostatic stresses in a plane, are strongly affected by the elastic characteristics of the material. of the plate under consideration.

In a flat plate with two holes loaded at its ends, the stress concentration interaction depends on the distance and the size ratio between them (Monroy & Godoy, 2006). Martínez, Carrera & Ferrer (2006) presents the study of a flat plate with a hole in the center, under the effects of a linear load gradient, they establish an approximate computational model that reduces the type of load required and supports the results obtained experimentally. by photoelasticity and numerically by using the software ANSYS®.

Noda & Takase (2006) analyze the stress concentration in a round bar with a circular arc or V-shaped notch that supports torsion, tension and bending loads, obtaining equations that allow determining the stress concentration in these pieces with an error of less than 1%. Susca, Bambill, Laura & Rossi (2006) analyze the stress concentration generated by a small rectangular hole with rounded edges in an orthotropic plate, observing that the greatest stress concentration factors are found in the main axis 1 which is at a angle of 67.5º with respect to the x-axis.

The theoretical stress concentration factor for parts made of orthotropic materials is significantly influenced by the type of applied load, as well as by known parameters such as the relative size of the hole.

ISSN: 2523-2428

In addition, the load that produces the greatest effects on the theoretical factors of stress concentration is the biaxial tension-tension load, whose effects are not very noticeable (Méndez & Torres, 2006). For his part, Sánchez (2006) analyzes the stress concentration in an orthotropic plate with an elliptical opening subjected to an axial load for a bone material taken from the diaphysis of the human tibia.

The reason for analyzing the elliptical opening and not the circular one is because the elliptical opening leads to a generalized analysis and in the limit, when the ratio of the semi-minor axis to the semi-major axis of the ellipse is very large, the hole tends to be a very large slot. thin (crack) and therefore its stress concentrator increases. The stress concentration factor in composite materials depends closely on the geometry of the piece, in addition to the fact that the stress concentration factor is not a sufficient value, by itself, for the prediction of failure in laminated materials (Domínguez, Santos, Robles & Ortega, 2006).

It is difficult to establish behavior parameters in orthotropic materials, but there is a marked influence between the relationships of the elastic constants and the stress concentration factors (Susca, Bambill & Rossit, 2007). Peñaranda, Pedroza & Méndez (2007) analyze the stress concentration in a plate of infinite length with two holes of equal radii, using finite element software, varying the distance between the centers of the two holes and their diameter. For their part, Gómez, Elices, Berto & Lazzarin (2008) study the stress concentration factor for U-shaped notches which support mixed loads using the concept based on the criterion of the average deformation of the energy density.

Sonmez (2009) carried out a study to optimize the shape of the fillets and reduce the stress concentration in flat and round bars subjected to axial loads, bending, torsion or combined loads. While Osorio, Rodríguez, Gámez & Ojeda (2010) studies the distribution of stresses produced by the effect of various loading conditions, in said study a numerical evaluation is carried out to analyze a plate for internal fixation of fractures occurring in the distal radius, the results show a concentration of stresses in the regions adjacent to the plate holes and in the screws located at the ends of the fixation plate.

Balankin, Susarrey, Mora Santos, Patiño, Yoguez, & García (2011) theoretically and experimentally study the effect of long-range correlations in the material microstructure on the stress concentration in the vicinity of the notch tip. According to the results obtained in experimental tests that they carry out, they obtain a good approximation of the effect of the size of the notch on the resistance to fracture of sheets of different types of paper.

Louhghalam, Igusa, Park, Choi & Kim (2011) present a model that is numerically coupled to the finite element method to determine the stresses at the corners of rectangular openings in plates subjected to bending. On the other hand, Sharma, Panchal & Patel (2011) analyze an infinite orthotropic plate with a circular hole subjected to internal pressure using the Mushkhelisvili method, finding that the orientation of the fibers and the stacking sequence have a significant effect on the distribution. stress around the hole.

While Sharma (2011) determines the stress concentration using Mushkhelisvili's method around circular, elliptical and triangular cutouts in infinite plates of laminated composite materials supporting arbitrary biaxial loads.

The stress concentration is one of the factors that contribute to reducing the life of a mechanical component subjected to fatigue (Khalil Abada, Pasinia & Cecereb, 2012). Dharmin, Khushbu & Chetan (2012) present a review of the research that has been carried out about stress analysis on infinite plates with cutouts. Many analytical, numerical, and experimental techniques are available to reduce the stress concentration factor around discontinuities. Different ways to determine the stress concentration factor in flat plates composed of different materials under different loading conditions have been reported (Nagpal, Jain & Sanyal, 2012).

ISSN: 2523-2428

In general, the maximum stress concentration for plates of finite width with a central hole under static axial load always occurs at the periphery of the hole, in addition, the stress concentration factor is maximum at the tip of the hole, that is, perpendicular to the load (Nagpal, Sanyal & Jain, 2013). Mohan Kumar, Rajest, Yogesh & Yeshaswini (2013) analyze the stress concentration in flat plates with circular, triangular, and rectangular holes, studying the variation of the stress concentration due to the hole geometry change. For their part, Henrique, Tácito & Moreno (2013) perform a finite element analysis to predict the elasto-plastic stress concentration factor for a 1020 steel alloy.

The use of modified elliptical shaped notches is suggested because it causes a lower stress concentration compared to semicircular notches and slots, the ratio of the minor and major axes of the ellipse should be between 0.3 and 0.4 (Ahsan, Prachurja, Ali & Mamun, 2013). On the other hand, Momcilovic, Motok & Maneski (2013) carry out an analysis of the stress concentration factor in the corner of an opening in a rectangular plate with small radii of curvature, using analytical, experimental, and finite element methods, making a comparison among the three methods.

Ortega, Garcia, Rocha & Guzmán (2013) show how to obtain stress concentration curves with the help of ANSYS® software. The determined stress concentration factors are plotted in a dimensionless way, obtaining stress concentrator curves.

The least squares method is used to fit the data from these curves to sixth degree polynomial equations with a value of R2 between 0.9987 and 1.

Darwisha, Tashtoushb & Gharaibehb (2013) study the in-plane stress concentration factor (SCF) in countersunk rivet holes in orthotropic rolled plates under uniaxial tensile loading. Finite element analysis is performed using ANSYS® software. The effect of various geometric and material parameters such as plate thickness, straight shank radius, countersink angle, countersink depth, plate width, and layer angles of SCF laminate are investigated.

Based on the results, it was found that the SCF values obtained by means of the formulated equation are within 7% of the finite element (FE) results for 96% of the runs and that the maximum overall error is less than 14%.

Ou, Lu, Cui & Lin (2013) show a shape optimization approach to minimize stress concentration and peaks caused by contact pressure. Their approach focuses on directly modifying the shape of the layers near the region where the stress concentration is measured by the Von Mises stresses and the contact surface measures the contact pressure. To evaluate the proposed approach, three case studies are presented, the results obtained show that the optimization of developed form is especially applicable to the design and analysis of multi-body systems where the limit stress concentration and contact pressure distribution are an important consideration.

Liu & Tang (2015) present a detailed analysis on stress concentration in composite materials reinforced with unidirectional notched fibers. Due to the formation of longitudinal splitting at the notch tips along the fiber direction, the extremely high stress concentrations ahead of the notch tip could be drastically reduced for composite materials under remote stress. The inability of the widely used material property degradation method to accurately redistribute local stresses at notch tips is examined.

The objective of this work is to analyze the stress concentration in a flat plate with two centered holes and subjected to an axial tension load.

A total of 125 simulations are carried out in a finite element software in order to find the maximum stress that the plate supports and subsequently determine the stress concentration factor, the results obtained are plotted for the W/D ratios of 1.2, 1.5, 2, 2.5 and 3 depending on the s/D ratio, finally the least squares method is applied to the values obtained to obtain equations that allow predicting the stress concentration factor for the analyzed case study.

ISSN: 2523-2428

All finite element

There are many facets of engineering in which it is necessary to determine the distribution of stresses and strains in an elastic continuum (Zienkiewicz, 1982). It is generally accepted that numerical analysis methods in engineering and applied sciences fall into three broad categories: finite differences, finite elements, and boundary elements (Cerrolaza, 2006).

Finite Element Analysis (FEA) has had a tremendous boost since the advent of the computer age. This has allowed the creation of multiple platforms to implement the theory of finite elements, of which Ansys is a particular example (Roa Garzón & Garzón Alvarado, 2002).

The finite element is a numerical method that is used for the modeling and simulation of problems in many fields of engineering, such as: structural analysis, heat transfer, fluid mechanics, electricity and magnetism, or a combination of them.

The term "finite element" expresses the idea that the object of study can be divided into a certain number of elements, with a defined mathematical model that can be represented in a matrix arrangement whose solution is obtained by applying the basic rules of linear algebra through of a computer program (Córdova Aquino & De Dios Domínguez, 2007)

There are two general approaches associated with the understanding and application of the finite element method. The first approach is called the force or flexibility method, which is based on the use of internal forces as the unknowns of the problem. To obtain the governing equations, the equilibrium equations have to be used first. Then it is necessary to introduce additional equations generated by the compatibility equations. The result is the array of redundant algebraic equations that determine the unknown internal forces. The second approach of the method is the displacement method, or stiffness method, which assumes the displacement of nodes as the unknowns of the problem (Pérez Mitre, 2004).

Fonseca Lopes (2011) mentions that regardless of the physical nature of the problem, its analysis using the Finite Element Method follows the following steps:

- Definition of the problem and its domain.
- Discretization of the domain.
- Identification of the state variable(s).
- Formulation of the problem.
- Establishment of reference systems.
- Construction of the functions of approximation of the elements.
- Determination of the equations at the level of each element.
- Transformation of coordinates.
- Assembling the equations of the elements.
- Introduction of the boundary conditions.
- Solution of the resulting set of simultaneous equations.
- Interpretation of the results.

In the present work, an eight-node quadrilateral element is used to perform the analysis in ANSYS®. Figure 1 shows a schematic of the eight-node quadrilateral element.

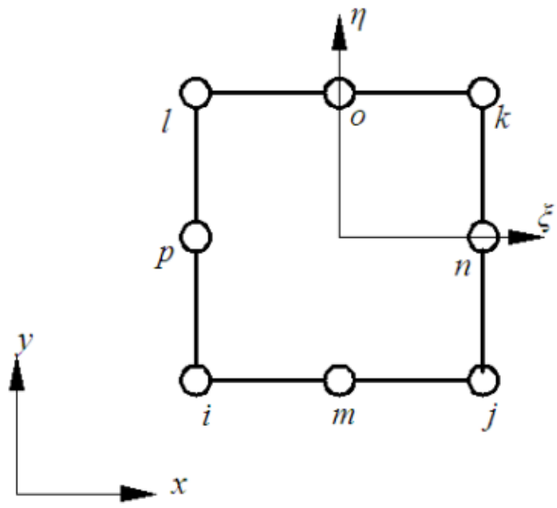

Figure 1 Schematic of the 8-mode quadrilateral element

Equations (1) through (8) are the shape functions of the nodes of the element in Figure 1 in terms of the local coordinates.

$$N_i = \frac{1}{4}(1-\xi)(1-\eta)(-\xi-\eta-1) \quad (1)$$

$$N_j = \frac{1}{4}(1+\xi)(1-\eta)(\xi-\eta-1) \quad (2)$$

$$N_k = \frac{1}{4}(1+\xi)(1+\eta)(\xi+\eta-1) \quad (3)$$

$$N_l = \frac{1}{4}(1-\xi)(1+\eta)(-\xi+\eta-1) \quad (4)$$

$$N_m = \frac{1}{2}(1-\xi^2)(1-\eta) \quad (5)$$

$$N_n = \frac{1}{2}(1+\xi)(1-\eta^2) \quad (6)$$

$$N_o = \frac{1}{2}(1-\xi^2)(1+\eta) \quad (7)$$

$$N_p = \frac{1}{2}(1-\xi)(1-\eta^2) \quad (8)$$

The partial derivatives of the global coordinates in terms of the local coordinates are presented in Equations (9) through (12).

$$\frac{\partial x}{\partial \xi} = \frac{\partial N_i}{\partial \xi}x_i + \frac{\partial N_j}{\partial \xi}x_j + \frac{\partial N_k}{\partial \xi}x_k + \frac{\partial N_l}{\partial \xi}x_l + \frac{\partial N_m}{\partial \xi}x_m + \frac{\partial N_n}{\partial \xi}x_n + \frac{\partial N_o}{\partial \xi}x_o + \frac{\partial N_p}{\partial \xi}x_p \quad (9)$$

$$\frac{\partial x}{\partial \eta} = \frac{\partial N_i}{\partial \eta}x_i + \frac{\partial N_j}{\partial \eta}x_j + \frac{\partial N_k}{\partial \eta}x_k + \frac{\partial N_l}{\partial \eta}x_l + \frac{\partial N_m}{\partial \eta}x_m + \frac{\partial N_n}{\partial \eta}x_n + \frac{\partial N_o}{\partial \eta}x_o + \frac{\partial N_p}{\partial \eta}x_p \quad (10)$$

$$\frac{\partial y}{\partial \xi} = \frac{\partial N_i}{\partial \xi}y_i + \frac{\partial N_j}{\partial \xi}y_j + \frac{\partial N_k}{\partial \xi}y_k + \frac{\partial N_l}{\partial \xi}y_l + \frac{\partial N_m}{\partial \xi}y_m + \frac{\partial N_n}{\partial \xi}y_n + \frac{\partial N_o}{\partial \xi}y_o + \frac{\partial N_p}{\partial \xi}y_p \quad (11)$$

$$\frac{\partial y}{\partial \eta} = \frac{\partial N_i}{\partial \eta}y_i + \frac{\partial N_j}{\partial \eta}y_j + \frac{\partial N_k}{\partial \eta}y_k + \frac{\partial N_l}{\partial \eta}y_l + \frac{\partial N_m}{\partial \eta}y_m + \frac{\partial N_n}{\partial \eta}y_n + \frac{\partial N_o}{\partial \eta}y_o + \frac{\partial N_p}{\partial \eta}y_p \quad (12)$$

The partial derivatives of the shape functions (Equations 1 to 8) with respect to the local coordinates are presented in Equations (13) to (28).

$$\frac{\partial N_i}{\partial \xi} = -\frac{1}{4}(1-\eta)(2\xi-\eta) \quad (13)$$

$$\frac{\partial N_i}{\partial \eta} = -\frac{1}{4}(1-\xi)(-2\eta-\xi) \quad (14)$$

$$\frac{\partial N_j}{\partial \xi} = \frac{1}{4}(1-\eta)(2\xi-\eta) \quad (15)$$

$$\frac{\partial N_j}{\partial \eta} = -\frac{1}{4}(1+\xi)(\xi-2\eta) \quad (16)$$

$$\frac{\partial N_k}{\partial \xi} = \frac{1}{4}(1+\eta)(2\xi+\eta) \quad (17)$$

$$\frac{\partial N_k}{\partial \eta} = \frac{1}{4}(1+\xi)(2\eta+\xi) \quad (18)$$

$$\frac{\partial N_l}{\partial \xi} = -\frac{1}{4}(1+\eta)(\eta-2\xi) \quad (19)$$

$$\frac{\partial N_l}{\partial \eta} = \frac{1}{4}(1-\xi)(2\eta-\xi) \quad (20)$$

$$\frac{\partial N_m}{\partial \xi} = -(1-\eta)\xi \quad (21)$$

$$\frac{\partial N_m}{\partial \eta} = -\frac{1}{4}(1-\xi^2) \quad (22)$$

$$\frac{\partial N_n}{\partial \xi} = \frac{1}{2}(1-\eta^2) \quad (23)$$

$$\frac{\partial N_n}{\partial \eta} = -\eta(1+\xi) \quad (24)$$

$$\frac{\partial N_o}{\partial \xi} = -\xi(1+\eta) \quad (25)$$

$$\frac{\partial N_o}{\partial \eta} = \frac{1}{2}(1-\xi^2) \quad (26)$$

$$\frac{\partial N_p}{\partial \xi} = -\frac{1}{2}(1-\eta^2) \quad (27)$$

$$\frac{\partial N_p}{\partial \eta} = -\eta(1-\xi) \quad (28)$$

Equations (29) and (30) are the partial derivatives of the shape functions with respect to the global coordinates.

ISSN: 2523-2428

$$\frac{\partial N_{i...p}}{\partial x}=\frac{1}{|J|}\left(\frac{\partial y}{\partial \eta}\frac{\partial N_{i...p}}{\partial \xi}-\frac{\partial y}{\partial \xi}\frac{\partial N_{i...p}}{\partial \eta}\right) \quad (29)$$

$$\frac{\partial N_{i...p}}{\partial y}=\frac{1}{|J|}\left(-\frac{\partial x}{\partial \eta}\frac{\partial N_{i...p}}{\partial \xi}+\frac{\partial x}{\partial \xi}\frac{\partial N_{i...p}}{\partial \eta}\right) \quad (30)$$

The Jacobian J is defined by equation (31).

$$|J|=\frac{\partial x}{\partial \xi}\frac{\partial y}{\partial \eta}-\frac{\partial x}{\partial \eta}\frac{\partial y}{\partial \xi} \quad (31)$$

The deformation matrix is defined by equation (32), while the shape function matrix is defined by equation (33).

$$B=\begin{bmatrix} \frac{\partial N_i}{\partial x} & 0 & \frac{\partial N_j}{\partial x} & 0 & \dots & \frac{\partial N_p}{\partial x} & 0 \\ 0 & \frac{\partial N_i}{\partial x} & 0 & \frac{\partial N_j}{\partial x} & \dots & 0 & \frac{\partial N_p}{\partial x} \\ \frac{\partial N_i}{\partial x} & \frac{\partial N_i}{\partial x} & \frac{\partial N_j}{\partial x} & \frac{\partial N_j}{\partial x} & \dots & \frac{\partial N_p}{\partial x} & \frac{\partial N_p}{\partial x} \end{bmatrix} \quad (32)$$

$$N=\begin{bmatrix} N_i & 0 & N_j & 0 & \dots & N_p & 0 \\ 0 & N_i & 0 & N_j & \dots & 0 & N_p \end{bmatrix} \quad (33)$$

The Gauss-Legendre quadrature is used to determine the stiffness matrix. The stiffness matrix of each element is defined by Equation (34).

$$K^e=K_{11}^e+K_{12}^e+K_{21}^e+K_{22}^e \quad (34)$$

Where:

$$K_{11}^e=tH_1^2J(\xi_1,\eta_1)B^T(\xi_1,\eta_1)DB(\xi_1,\eta_1) \quad (35)$$

$$K_{12}^e=tH_1H_2J(\xi_1,\eta_2)B^T(\xi_1,\eta_2)DB(\xi_1,\eta_2) \quad (36)$$

$$K_{21}^e=tH_2H_1J(\xi_2,\eta_1)B^T(\xi_2,\eta_1)DB(\xi_2,\eta_1) \quad (37)$$

$$K_{22}^e=tH_2^2J(\xi_2,\eta_2)B^T(\xi_2,\eta_2)DB(\xi_2,\eta_2) \quad (38)$$

Equations (1) through (38) define a square element with eight nodes.

Stress concentration

Most real machine parts will have variable cross sections. will have varying cross sections.

For example, shafts are often staggered at different diameters to accept different diameters in order to accept bearings, gears, pulleys, etc. bearings, gears, pulleys, etc. A shaft may have slots for circular keyways, or for rings, or have for rings, or have wedges or holes for the attachment of other other parts. Bolts are bolts are threaded with heads larger than their shank. Any of these changes in the geometry of the cross-section geometry can cause localized stress concentrations (Norton, 1999).

The analysis of geometric shapes to determine to determine stress concentration factors becomes a difficult stress concentration factor becomes a difficult problem and not many solutions are found.

Most stress concentrators are determined by experimental techniques. Although the finite element method has been used, the fact that the elements are, in effect, finite, prevents finding the actual maximum stress. Generally, experimental approaches include photoelasticity, meshing methods, brittle coating methods and electrical methods with strain gauges (Budynas & Keith Nisbett, 2008). Mott (2006) mentions that stress concentration factors should always be used when analyzing elements under fatigue loading, because fatigue cracks usually initiate near points of high local tensile stress.

Methodology

The proposed case study consisted of study the stress concentration in a flat plate with two flat plate with two aligned and centered holes which supports axial load, we use the finite element software the finite element software ANSYS®, is used to study the stress concentration in a flat plate with two aligned and centered holes. software is used, in order to the modeling in this software, an eight-node square element is used the modeling in this software uses an eight-node square element, of which four nodes correspond to each corner of the quadrilateral of the quadrilateral and the other four nodes are intermediate nodes. four nodes are intermediate nodes. The most suitable element for such an analysis is therefore the Solid 8 element. analysis is therefore the Solid 8 node element 183.

ISSN: 2523-2428

This element is used because it is a quadrilateral with intermediate nodes at this element is used because it is a quadrilateral with intermediate nodes on the edges, so it tends to deform and couple easily during meshing in a curved section. This element is configured to work as a plane stress element with thickness. In the elaboration of the simulations an isotropic material is used, which is assigned the properties of low carbon steel, elastic modulus of 210 GPa, Poisson's ratio of 0.28.

The developed models support a tensile load at one end, while at the other end they are restrained in the x-direction.

Figure 2 presents the flat rectangular plate with two centered holes to be analyzed, which has the following characteristics:

- Plate length (L) of 0.3 m.
- Applied force (F) of 100 kN.
- Plate thickness of 0.01 m.

The width of the plate (W), the distance between hole centers (s) and the diameter of the holes (D) are variable and change in each analysis.

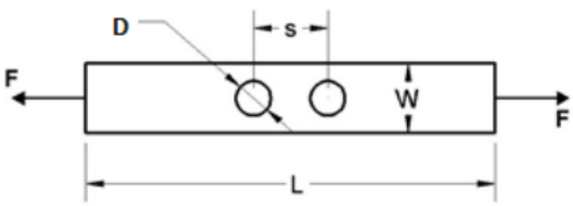

Figure 2 Flat plate with two boreholes to be analyzed

Figure 3 presents the model made in the software for the case study.

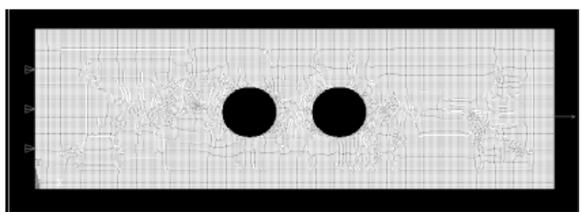

Figure 3 Model created to analyze the study case

A total of 125 simulations are performed to obtain σmax and subsequently obtain the value of Kt, the simulations are distributed as follows:

- 25 simulations for the case W/D = 3.
- 25 simulations for the case W/D = 2.5.
- 25 simulations for the W/D = 2 case.
- 25 simulations for the case W/D = 1.5.
- 25 simulations for the case W/D = 1.2.

The simulations are performed by modifying the value of W in ranges of 0.004 m, starting at 0.096 m and ending at 0.002 m. The value of s is determined by adding the value of D to 0.02; that is, for all cases, the separation between the closest surfaces of the boreholes is assumed to be 0.02 m. The value of D is determined using Equation (39), in this equation h takes the value of 1.2, 1.5, 2, 2.5 and 3 depending on the case analyzed.

$$\frac{W}{D} = h \tag{39}$$

To obtain the value of K_t, σ_{max} is divided by $\sigma_{theoretical}$ (Equation 40).

$$K_t = \frac{\sigma_{max}}{\sigma_{teórico}} \tag{40}$$

The stress $\sigma_{theoretical}$ is obtained by means of equation (41), in this equation the value of the area is determined at the place where the cross-section of the cross-section of the part is minimum.

$$\sigma_{teorico} = \frac{F}{A} \tag{41}$$

Results

The Kt values obtained for the five W/D ratios are plotted as a function of the dimensionless S/D ratio, the graph obtained is presented in Figure 4.

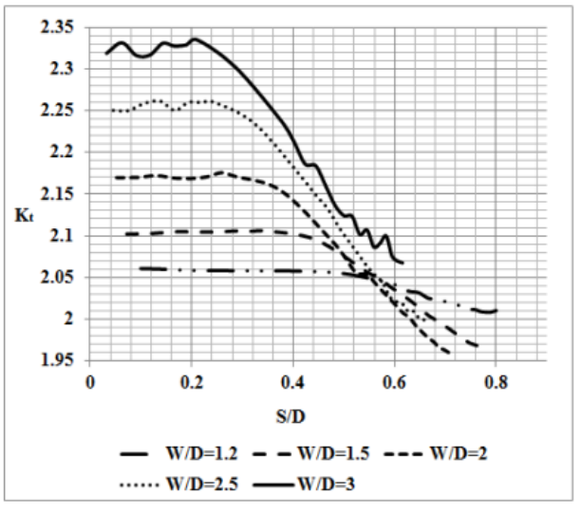

Figure 4 Stress concentration factor plot for a flat plate with two holes subjected to axial loading.

To the K_t values obtained for the W/D ratios of 1.2, 1.5, 2, 2.5 and 3 which are shown graphically in Figure 4, the least squares method is applied to obtain a set of linear equations (Equations 42 to 46), a set of exponential equations (Equations 47 to 51), a set of second-degree polynomial equations (Equations 52 to 56) and finally a set of sixth degree polynomial equations (Equations 57 to 58).

Figure 5 shows graphically the lines obtained for the linear regression using the least squares method using the least squares method and equations (42) to (46) represent the linear equations obtained for the case study analyzed.

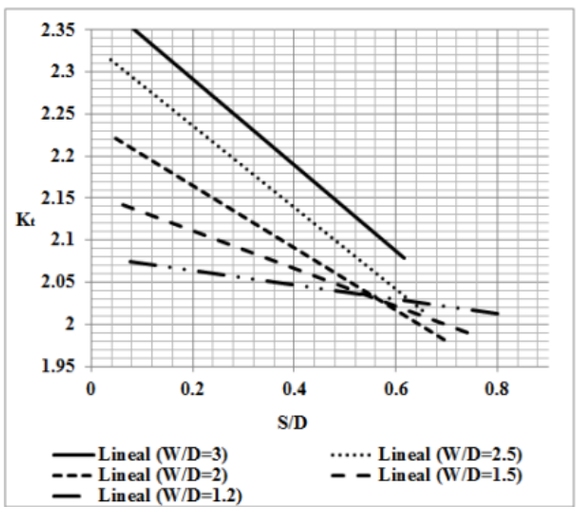

Figure 5 Linear regression plot obtained using the least squares method

Equation (42) is the linear equation for W/D=1.2 and has a value of $R^2 = 0.9354$.

$$K_t = -0.5136\left(\frac{s}{D}\right) + 2.3942 \qquad (42)$$

Equation (43) is the linear equation for W/D=1.5 and has a value of $R^2 = 0.925$.

$$K_t = -0.4846\left(\frac{s}{D}\right) + 2.3325 \qquad (43)$$

Equation (44) is the linear equation for W/D=2 and has a value of $R^2 = 0.9183$.

$$K_t = -0.3691\left(\frac{s}{D}\right) + 2.2392 \qquad (44)$$

Equation (45) is the linear equation for W/D=2.5 and has a value of $R^2 = 0.8835$.

$$K_t = -0.2241\left(\frac{s}{D}\right) + 2.1555 \qquad (45)$$

Equation (46) is the linear equation for W/D=3 and has a value of $R^2 = 0.8835$. for W/D=3 and has a value of $R^2 = 0.8884$.

$$K_t = -0.0859\left(\frac{s}{D}\right) + 2.0813 \qquad (46)$$

Figure 6 shows graphically the lines obtained for the exponential regression using the least squares method, equations (47) to (51) are the exponential equations obtained for the case study analyzed.

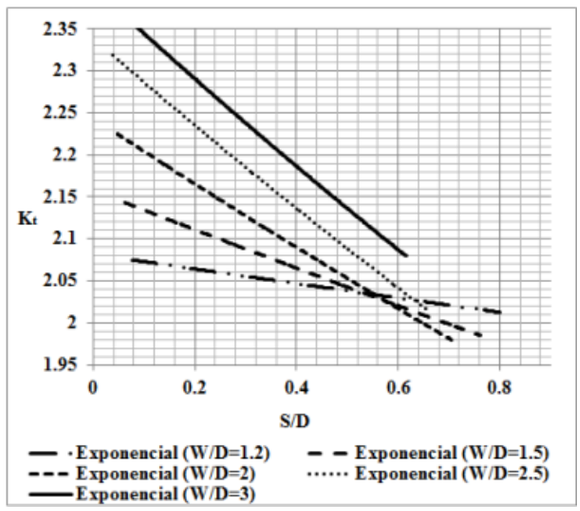

Figure 6 Exponential regression graph obtained using the least squares method

Equation (47) is the exponential equation for W/D = 1.2 and has a value of $R^2 = 0.9332$.

$$K_t = 2.3997e^{-0.233\left(\frac{s}{D}\right)} \qquad (47)$$

Equation (48) is the exponential equation for W/D = 1.5 and has a value of $R^2 = 0.9217$.

$$K_t = 2.3388e^{-0.227\left(\frac{s}{D}\right)} \quad (48)$$

Equation (49) is the exponential equation for W/D = 2 and has a value of $R^2 = 0.9152$.

$$K_t = 2.2439e^{-0.178\left(\frac{s}{D}\right)} \quad (49)$$

Equation (50) is the exponential equation for W/D = 2.5 and has a value of $R^2 = 0.881$.

$$K_t = 2.1578e^{-0.11\left(\frac{s}{D}\right)} \quad (50)$$

Equation (51) is the exponential equation for W/D = 3 and has a value of $R^2 = 0.8874$.

$$K_t = 2.0817e^{-0.042\left(\frac{s}{D}\right)} \quad (51)$$

Figure 7 shows graphically the lines obtained for the second-degree polynomial regression using the least squares method, equations (52) to (56) are the second-degree polynomial equations obtained for the case study analyzed.

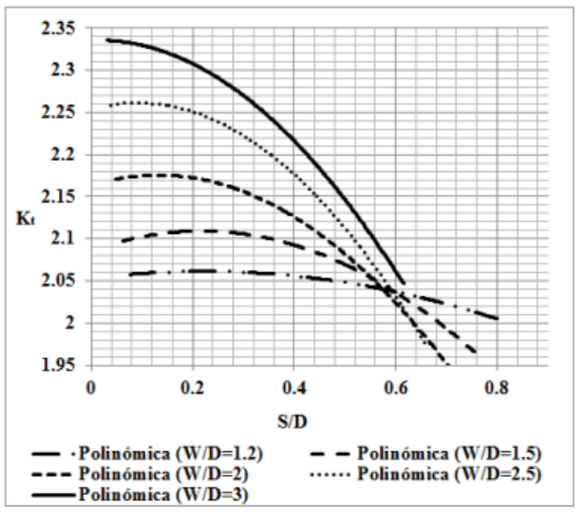

Figure 7 Plot of second-degree polynomial regression obtained by the least square's method. squares method

$$K_t = -0.7972\left(\frac{s}{D}\right)^2 + 0.0207\left(\frac{s}{D}\right) + 2.3357 \quad (52)$$

Equation (52) is the second-degree polynomial second degree polynomial equation for W/D = 1.2 and has a value of $R^2 = 0.9761$.

$$K_t = -0.8855\left(\frac{s}{D}\right)^2 + 0.1596\left(\frac{s}{D}\right) + 2.2542 \quad (53)$$

Equation (53) is the second degree polynomial equation for W/D = 1.5 and has a value of $R^2 = 0.9871$.

$$K_t = -0.6943\left(\frac{s}{D}\right)^2 + 0.1847\left(\frac{s}{D}\right) + 2.1633 \quad (54)$$

Equation (54) is the second-degree polynomial equation for W/D = 2 and has a value of $R^2 = 0.9918$.

$$K_t = -0.4954\left(\frac{s}{D}\right)^2 + 0.2151\left(\frac{s}{D}\right) + 2.0858 \quad (55)$$

Equation (55) is the second-degree polynomial equation for W/D = 2.5 and has a value of $R^2 = 0.9949$.

$$K_t = -0.1679\left(\frac{s}{D}\right)^2 + 0.0742\left(\frac{s}{D}\right) + 2.0531 \quad (56)$$

Equation (56) is the second-degree polynomial equation for W/D = 3 and has a value of $R^2 = 0.9842$.

Figure 8 shows graphically the lines obtained by the sixth-degree polynomial regression using the least squares method, equations (57) to (61) are the sixth degree polynomial equations obtained for the case study analyzed.

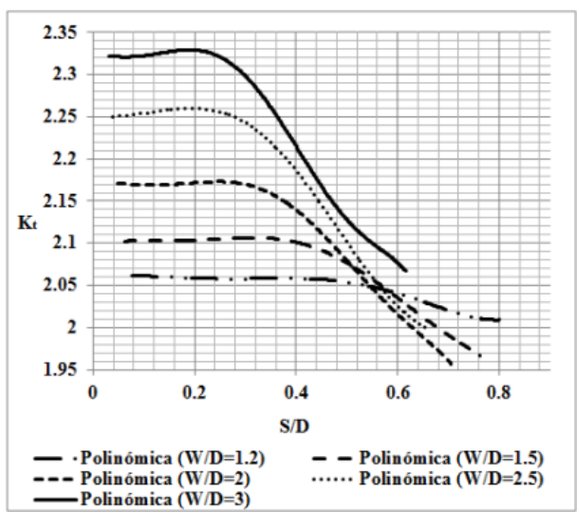

Figure 8 Sixth degree polynomial regression graph obtained by the least square's method

$$K_t = -152.39\left(\frac{s}{D}\right)^6 + 257.58\left(\frac{s}{D}\right)^5 - 146.04\left(\frac{s}{D}\right)^4 + \\ +29.371\left(\frac{s}{D}\right)^3 - 1.5742\left(\frac{s}{D}\right)^2 - 0.0281\left(\frac{s}{D}\right) + 2.3236 \quad (57)$$

Equation (57) is the sixth-degree polynomial equation for W/D = 1.2 and has a value of $R^2 = 0.9964$.

$$K_t = -36.163\left(\frac{s}{D}\right)^6 + 72.68\left(\frac{s}{D}\right)^5 - 46.463\left(\frac{s}{D}\right)^4 + \\ +9.0564\left(\frac{s}{D}\right)^3 - 0.4102\left(\frac{s}{D}\right)^2 + 0.0417\left(\frac{s}{D}\right) + 2.249 \quad (58)$$

Equation (58) is the sixth-degree polynomial equation for W/D = 1.5 and has a value of $R^2 = 0.9992$.

$$K_t = -58.154\left(\frac{s}{D}\right)^6 + 124.53\left(\frac{s}{D}\right)^5 - 95.65\left(\frac{s}{D}\right)^4 + \\ +31.014\left(\frac{s}{D}\right)^3 - 4.3635\left(\frac{s}{D}\right)^2 + 0.2469\left(\frac{s}{D}\right) + 2.1656 \quad (59)$$

Equation (59) is the sixth-degree polynomial equation for W/D = 2 and has a value of $R^2 = 0.9988$.

$$K_t = -22.527\left(\frac{s}{D}\right)^6 + 59.696\left(\frac{s}{D}\right)^5 - 58.529\left(\frac{s}{D}\right)^4 + \\ +25.902\left(\frac{s}{D}\right)^3 - 5.4764\left(\frac{s}{D}\right)^2 + 0.537\left(\frac{s}{D}\right) + 2.0842 \quad (60)$$

Equation (60) is the sixth-degree polynomial equation for W/D = 2.5 and has a value of $R^2 = 0.9997$.

$$K_t = 0.0486\left(\frac{s}{D}\right)^6 + 4.7388\left(\frac{s}{D}\right)^5 - 9.1404\left(\frac{s}{D}\right)^4 + \\ +5.9017\left(\frac{s}{D}\right)^3 - 1.5939\left(\frac{s}{D}\right)^2 + 0.1628\left(\frac{s}{D}\right) + 2.0557 \quad (61)$$

Equation (61) is the sixth-degree polynomial equation for W/D = 3 and has a value of $R^2 = 0.9984$.

Conclusions

The results obtained show that the stress concentration factor decreases as the s/D ratio increases, at the same time the stress concentration factor decreases when the W/D ratio also decreases.

The linear equations obtained by the least square's method do not provide a good approximation because the R2 values vary between 0.9354 and 0.8835, therefore they do not adjust adequately to the values obtained, it is not recommended to use these equations, only if it is desired to obtain a quick approximation of the stress values supported by the part.

On the other hand, the exponential equations obtained do not have a good approximation to the approximation to the values of the stress concentration factor obtained. stress concentration factor values obtained. The values of R 2 values vary between 0.9332 and 0.8810, so it is not also recommended to use these equations to predict the stress concentration factor. stress concentration factor.

The polynomial equations of second the second-degree polynomial equations obtained attach well to the calculated stress concentration factor values. of the calculated stress concentration factor. The R2 values for these equations vary between 0.9761 and 0.9949, therefore, these equations provide reliable values of the stress concentration factor for the mechanical part under study.

On the other hand, the sixth-degree polynomial equations determined strongly fit the stress concentration factor values obtained. These equations have a value of R2 that varies between 0.9964 and 0.9997, therefore the values of the stress concentration factor for the analyzed case study can be determined by these equations since the obtained values strongly fit the data calculated with the help of the finite element software.

References

Ahsan R. U., Prachurja P., Ali A. R. M. & Mamun M. A. H. (2013). Determination of effect of elliptic notches and grooves on stress concentration factors on notched bar in tension and grooved shaft under torsion. Journal of Naval Architecture and Marine Engineering. 10(1). pp. 25-32.

ISSN: 2523-2428

Balankin A., Susarrey O., Mora Santos C., Patiño J., Yoguez A., & García E. (2011). Stress concentration and size effect in fracture of notched heterogeneous material. Physical review E statistical, nonlinear, and soft matter physics. 83(1).

Bambill D. V., Susca A., Laura P. A. & Maíz S. (2005). Concentración de tensiones en placa ortótropa sometida a esfuerzo biaxial, Mecánica Computacional. 24(1). pp. 2675-2694.

Budynas R. G. & Keith Nisbett G. (2008). Diseño en ingeniería mecánica de Shigley. McGrawHill. Cerrolaza M. (2006). El metodo de los elementos finitos para ingenieria y ciencias aplicadas: teoría y programas. Universidad Central de Venezuela, Consejo de desarrollo científico y humanístico.

Darwisha F.,Tashtoushb G. & Gharaibehb M. (2013). Stress concentration analysis for countersunk rivet holes in orthotropic plates. European Journal of Mechanics - A/Solids. 37(1). pp. 69-78.

Dharmin P., Khushbu P. & Chetan J. (2012). A Review on Stress Analysis of an Infinite Plate with Cut-outs‖, International Journal of Scientific and Research Publications. 2(11). pp. 1-7.

Da Fonseca Lopes Z. A. (2011) El método de los elementos finitos: una introducción. Universidad Rafael Urdaneta, Fondo Editorial Biblioteca.

Domínguez P. N., Santos R. D., Robles S. I. & Ortega N. F. (2006). Concentración de tensiones en piezas de materiales compuestos. Mecánica Computacional. 25(1). pp. 537-548.

Gómez F. J., Elices M., Berto F. & Lazzarin P. (2008). A generalised notch stress intensity factor for U-notched components loaded under mixed mode. Engineering Fracture Mechanics. 75(1). pp. 4819–4833.

Henrique S., Tácito A. & Moreno M. E. (2013). Stress concentration factor calculation for a notched specimen under elasto-plastic loading. 22nd International Congress of Mechanical Engineering (COBEM 2013). pp. 7761-7769.

Khalil Abada E. M., Pasinia D. & Cecereb R. (2012). Shape optimization of stress concentration-free lattice for self-expandable Nitinol stent-grafts. Journal of Biomechanics. 45(6). pp. 1028–1035.

Liu G. & Tang K. (2015). Study on stress concentration in notched cross-ply laminates under tensile loading. Journal of composite materials. Journal of Composite Materials.

Louhghalam A., Igusa T., Park C., Choi S. & Kim K. (2011). Analysis of stress concentrations in plates with rectangular openings by a combined conformal mapping – Finite element approach. International Journal of Solids and Structures. 48(1). pp 1991-2004.

Maíz S., Rossi R. E., Laura P. A. & Bambill D. V. (2004). Efectos de la ortotropía sobre el factor de concentración de tensiones: extensión del problema de kirsch. Mecánica Computacional. 23(1). pp. 673-692.

Martínez J. E., Carrera J. & Ferrer L. A. (2006). Análisis experimental y numérico de esfuerzos en placas con orificio circular bajo el gradiente de carga lineal. Ingeniería mecánica, tecnología y desarrollo. 2(2).

Méndez J. I. & Torres J. I. (2006). Concentración de esfuerzo en una placa de material ortotrópico con una abertura elíptica. Congreso iberoamericano de metalurgia y materiales, Habana Cuba.

Mohan Kumar M., Rajest S., Yogesh H. & Yeshaswini B. R. (2013). Study on the effect of stress concentration on cutout orientation of plates with various cutouts and bluntness‖, International Journal of Modern Engineering Research. 3(3). pp. 1295-1303.

Momcilovic N., Motok M. & Maneski T. (2013). Stress concentration on the contour of a plate opening: analytical, numerical and experimental approach. Journal of theoretical and applied mechanics. 51(4). pp. 1003-1012.

Monroy H. A. & Godoy L. A. (2006). Un sistema computacional para la simulación de interacción de defectos estructurales. Mecánica computacional. 25(1), pp. 1-9.

ISSN: 2523-2428

Mott R. L. (2006). Diseño de elementos de máquinas. Pearson Education. Nagpal S., Jain N. & Sanyal S. (2012). Stress Concentration and Its Mitigation Techniques in Flat Plate with Singularities - A Critical Review. Engineering journal. 16(1).

Nagpal S., Sanyal S. & Jain N. K. (2013). Analysis and mitigation of stress concentration factor of a rectangular isotropic and orthotropic plate with central circular hole subjected to inplane static loading by design optimization. International Journal of Innovative Research in Science, Engineering and Technology IJIRSET. 2(6). pp. 2903-2913.

Noda N. A. & Takase Y. (2006). Stress concentration formula useful for all notch shape in a round bar (comparison between torsion, tension and bending). International Journal of Fatigue. 28(1). pp. 151-163.

Norton R. L. (1999). Diseño de Máquinas. Prentice Hall. Osorio A., Rodríguez D., Gámez B. & Ojeda D. (2010). Análisis numérico de una placa para fijación de fracturas de radio distal utilizando el método de elementos finitos, Ingeniería UC. 17(1). pp. 28-36.

Ortega F. J., Garcia J. M., Rocha G. y Guzmán A. (2013). Análisis de esfuerzos en placas planas sometidas a carga axial‖, Memorias del XIX Congreso Internacional Anual de la SOMIM. pp. 478-487.

Ou H., Lu B., Cui Z. S., Lin C. (2013). A direct shape optimization approach for contact problems with boundary stress concentration. Journal of Mechanical Science and Technology. 27(9), pp 2751-2759.

Peñaranda M., Pedroza J. B. & Méndez J. I. (2007). Determinación del factor teórico de concentración de esfuerzo de una placa infinita con doble agujero. 8 Congreso Iberoamericano de Ingeniería Mecánica, Cusco Perú.

Pérez Mitre A. J. (2004). Análisis y optimización con interacción de Dummy, de la carrocería del automóvil "Tubolare SAND CAR" de Tecnoidea SA de CV, en impacto frontal empleando el método de elementos finitos en ALGOR FEA, mediante la simulación de eventos mecánicos. (Tesis de licenciatura, Universidad de las Américas Puebla). Recuperado de http://catarina.udlap.mx/u_dl_a/tales/documentos/lim/jimenez_p_a/portada.html

Roa Garzón M. A. & Garzón Alvarado D. A. (2002). Introducción al modelamiento por elementos finitos con Ansys. Departamento de Ingeniería Mecánica y Mecatrónica, Facultad de Ingeniería, Universidad Nacional de Colombia.

Roldan F. & Bastidas U. (2002). Estudio experimental y por análisis de elementos finitos del factor de concentrador de esfuerzo producido por un agujero en una placa plana. Dyna. 69(137). pp. 1-8.

Sánchez M. (2006). Factor teórico de concentración de esfuerzos en placas anisotrópicas. Departamento de Ingeniería Mecánica, UNEXPO Vicerrectorado Puerto Ordaz, Venezuela.

Sharma D. S. (2011). Stress Concentration around Circular/Elliptical/Triangular Cutouts in Infinite Composite Plate. Proceedings of the World Congress on Engineering. 3(1).

Sharma D. S., Panchal B. & Patel C. (2011). A General Solution for the Stresses around Internally Pressurized Circular hole in Symmetric Laminates. International Conference on Current Trends in Technology (NUiCONE–2011). pp. 1-5.

Sonmez F. O. (2009). Optimal shape design of shoulder fillets for flat and round bars under various loadings‖, Journal of mechanical engineering science. 223(1). pp. 1741-1754.

Susca A., Bambill D. V., Laura P. A. & Rossi R. E. (2006). Factor de concentración de tensiones en el entorno de un orificio rectangular presente en una placa ortótropa. Mecánica computacional. 25(1). pp. 411-427.

ISSN: 2523-2428

Susca A., Bambill D. V. & Rossit C. A. (2007). Análisis de la concentración de tensiones en placas ortótropas con orificio circular sometidas simultáneamente a cargas normales y tangenciales. Mecánica computacional. 26(1). pp. 386-405.

Zheng M. & Niemi E. (1997). Analysis of the stress concentration factor for a shallow notch by the slip-line field method. International Journal of Fatigue, Vol. 19, No. 3, pp. 191- 194, 1997.

Zienkiewicz O. C. (1982). El método de los elementos finitos. Editorial Reverte.

ISSN: 2523-2428